

# The oral bioavailability and metabolism of midazolam in stable critically ill children: a pharmacokinetic microtracing study

Bianca D van Groen, Elke HJ Krekels, Miriam G Mooij, Esther van Duijn, Wouter HJ Vaes, Albert D Windhorst, Joost van Rosmalen, Stan JF Hartman, N Harry Hendrikse, Birgit CP Koch, Karel Allegaert, Dick Tibboel, Catherijne AJ Knibbe, Saskia N de Wildt

*Submitted*

## ABSTRACT

Midazolam is metabolized by the developmentally regulated intestinal and hepatic drug metabolizing enzyme cytochrome P450 (CYP) 3A4/5. It is frequently administered orally to children, yet knowledge is lacking on the oral bioavailability in term neonates up until 1 year of age. Furthermore, the dispositions of the major metabolites 1-OH-midazolam (OHM) and 1-OH-midazolam-glucuronide (OHMG) after oral administration are largely unknown for the entire pediatric age span. We aimed to fill these knowledge gaps with a pediatric [ $^{14}\text{C}$ ]midazolam microtracer population pharmacokinetic study. Forty-six stable, critically ill children (median age 9.8 [range 0.3 – 276.4] weeks) received a single oral [ $^{14}\text{C}$ ]midazolam microtracer (58 [40-67] Bq/kg) when they received a therapeutic continuous intravenous midazolam infusion and had an arterial line in place enabling blood sampling. For midazolam, in a one-compartment model, bodyweight was a significant predictor for clearance (0.98 L/h) and volume of distribution (8.7L) (values for a typical individual of 5 kg). The typical oral bioavailability in the population was 66% (range 25%-85%). The exposures of OHM and OHMG were highest for the youngest age groups and significantly decreased with postnatal age. The oral bioavailability of midazolam, largely reflective of intestinal and hepatic CYP3A activity, was on average lower than the reported 49-92% for preterm neonates, and higher than the reported 21% for children >1 year of age and 30% for adults. As midazolam oral bioavailability varied widely, systemic exposure of other CYP3A-substrate drugs after oral dosing in this population may also be unpredictable, with risk of therapy failure or toxicity.

## INTRODUCTION

Midazolam is a short-acting benzodiazepine that is widely used in pediatric hospital practice for various indications, including the induction of anesthesia by oral administration.<sup>1, 2</sup> When an orally administered drug is subject to intestinal and/or hepatic drug metabolism, variation in its metabolism is an important determinant of bioavailability and systemic clearance of that drug.

Oral bioavailability is defined as the fraction of the administered oral dose reaching the systemic circulation unchanged and importantly depends on the absorption and first-pass metabolism by both intestinal and hepatic drug metabolizing enzymes. Cytochrome P450 (CYP) 3A is a drug metabolizing enzyme family, abundant in both the liver and the gut, which contributes to the first-pass metabolism of many orally administered drugs.<sup>3</sup> CYP3A consists of the three main isoforms CYP3A4, -3A5 and -3A7, for which the substrate specificity differs.<sup>3, 4</sup> *In vitro* studies have shown that the CYP3A7 abundance in the liver declines rapidly after birth and that the abundance CYP3A4 in the liver and in the gut increases with increasing age.<sup>5-7</sup> CYP3A5 is polymorphically expressed, with a stable expression from fetus to adult. This developmental pattern of CYP3A4 expression seen in *in vitro* studies is supported by pharmacokinetic (PK) data of CYP3A substrate drugs. The benzodiazepine midazolam is a well-validated CYP3A probe with substrate specificity for CYP3A4/5 and almost none for CYP3A7.<sup>8, 9</sup> In preterm infants (gestational age 26-31 weeks and postnatal age 3-13 days), oral midazolam clearance was markedly lower (0.16 L/h/kg vs 3.0 L/h/kg) and oral bioavailability higher (49-92% vs 21%) than in children beyond 1 year of age.<sup>10-12</sup> These findings suggest developmentally lower intestinal and/or hepatic CYP3A activity in preterm neonates. Midazolam is one of the many CYP3A4/5 substrates frequently administered to children.<sup>3</sup> Hence, this developmental pattern in CYP3A4/5 mediated systemic and pre-systemic metabolism may imply that safe and effective systemic exposure of oral doses of not only midazolam, but also other CYP3A4/5 substrates, may not be reached.

The oral bioavailability of midazolam has been previously studied across the pediatric age span.<sup>10-14</sup> However, there is a distinct knowledge gap for the age group from birth (term born) throughout infancy, i.e. <1-year-old. The classical study design to obtain data on oral bioavailability entails a cross-over study in which an oral and IV dose of a drug are administered alternately, with a wash-out period in between. This design is ethically and practically challenging as children are exposed twice to therapeutic drug doses with extensive blood sampling.

An interesting approach to study oral bioavailability is by a [ $^{14}\text{C}$ ]labelled microtracer, which has been shown practically and ethically feasible to study developmental changes in PK in children.<sup>15-17</sup> A microtracer is defined as ' $<1/100\text{th}$  of the dose needed to reach the no observed adverse effect level (NOAEL) or  $<100\text{ }\mu\text{g}$ ', concurrently administered with a therapeutic dose.<sup>18, 19</sup> The [ $^{14}\text{C}$ ]label allows quantification of extremely low plasma concentrations by accelerator mass spectrometry (AMS) in only 10-15  $\mu\text{l}$  plasma.<sup>20, 21</sup> A microtracer of an oral [ $^{14}\text{C}$ ]labelled drug is administered simultaneously with therapeutic IV doses of the same unlabeled drug, allowing measuring both the oral and IV disposition in one subject at the same time and, with that, accurately quantifying the absolute oral bioavailability<sup>15, 16</sup>, overcoming the limitations of a traditional cross-over design.

Besides the oral bioavailability of midazolam, the systemic exposure to the major metabolites 1-OH-midazolam (OHM) and 1-OH-midazolam-glucuronide (OHMG) after oral dosing is also of interest, since both metabolites are pharmacologically active, although to a lesser extent than midazolam.<sup>22</sup> Also, a better understanding of age-related variation in metabolite disposition provides further insight in developmental pharmacology. OHM is the primary metabolite formed by CYP3A, which is further glucuronidated to OHMG by UDP-glucuronosyltransferase (UGT) 2B4, -2B7 and, to a lesser extent, -1A4.<sup>23, 24</sup> A high systemic exposure to OHMG may result in therapeutic effects of this metabolite despite its lower potency.<sup>25</sup> A report of five critically ill adults with severe renal failure showed accumulation of OHMG after continuous IV infusion of midazolam.<sup>25</sup> This accumulation led to prolonged sedation (assessed by Ramsey score and electroencephalographic [EEG] evaluation) that could be reversed by the use of flumazenil, which is a competitive benzodiazepine antagonist. This finding highlights the importance of knowledge on disposition of the metabolites of midazolam. The metabolism and disposition of midazolam and the primary metabolite OHM after oral dosing have been described in preterm neonates and older children<sup>10, 13, 14, 26, 27</sup>, but gaps remain for term neonates to children  $<2$  years old. Most importantly, to the best of our knowledge, data on systemic exposure of OHMG in adults and children after oral dosing are not available.

Given these considerations, we have designed and conducted an oral [ $^{14}\text{C}$ ]midazolam microtracer population PK study in stable, critically ill children from 0-6 years old with the aim to answer two questions: (1) what is the oral bioavailability of midazolam; and (2) what is the systemic exposure to midazolam and its major metabolites OHM and OHMG after oral dosing in this population.

## MATERIAL AND METHODS

### Setting

This multicenter study was carried out in the level III pediatric intensive care unit (PICU) of the Erasmus MC–Sophia Children’s Hospital, Rotterdam, the Netherlands (October 2015–March 2018) and the Radboudumc–Amalia Children’s Hospital, Nijmegen, the Netherlands (May 2017–March 2018). The study was approved by the Dutch Central Committee on Research Involving Human Subjects (EudraCT 2014-003269-46). Parental written informed consent was obtained. The radiation exposure of a single microtracer was explained to the parents and legal guardians by a comparison with the yearly mean background exposure of 2.6 mSv in the Netherlands in 2013.<sup>28</sup> The Dutch Nuclear Research and Service Group estimated the radiation exposure for a single microtracer <1 µSv was well below the minimal risk category 1 of the International Commission of Radiological Protection, where a maximum exposure of 100 µSv is allowed. Category 1 risk studies are considered minimal risk and ethically justified in humans when they provide new scientific knowledge.<sup>29</sup>

### Population

Children were eligible to participate in the study when aged from birth (post menstrual age >36 weeks) up to 6 years of age, had medical need for sedation with continuous IV midazolam, and had an indwelling arterial or central venous line in place enabling blood sampling. To minimize inter-individual variability due to critical illness or organ failure, exclusion criteria were death anticipated in 48 hours, extra corporeal membrane oxygenation (ECMO) treatment, circulatory failure (defined by the administration of >1 vasopressor drug, or increase of the dose of a vasopressor drug in the last 6 hours), kidney failure (according to the pediatric Risk, Injury, Failure, Loss, End stage renal disease (pRIFLE) criteria ‘failure’, i.e. estimated creatinine clearance decreased by 75% or an urine output of <0.3 ml/kg/h for 24h or anuria for 12 hours), liver failure (defined by aspartate-aminotransferase [ASAT] or alanine-aminotransferase [ALAT] >2 times the upper limit for age), gastrointestinal disorders, or concomitant administration of co-medication known to interact with midazolam (according to the Flockhart Table<sup>TM30</sup>).

### Study design

A single [<sup>14</sup>C]midazolam (20.3 [14.1–23.6] ng/kg; 58 [40–67] Bq/kg; 0.25 ml/kg) dose was administered as an oral microtracer via the enteral feeding tube to ensure delivery in the gastrointestinal tract, followed by either 1–2 mL of saline or food to ensure rinsing of the tube. The IV therapeutic midazolam dose was prescribed by the treating physician for clinical purposes and was adjusted on the guidance of validated sedation scores and according to a standardized sedation titration protocol. According to this

protocol, midazolam bolus doses varied between 0.05-0.2 mg/kg and the continuous infusion rate between 0.05-0.3 mg/kg/h. Blood samples were taken pre-microtracer administration and around 0.5h, 1h, 2h, 4h, 6h, 12h, and 24h after administration of the [ $^{14}\text{C}$ ]midazolam microtracer to ensure that the PK of the oral absorption phase was captured. The maximum number of blood samples for the study was limited to 8 per subject and the maximum amount of blood could not exceed the guidelines by EMA (up to 1% of calculated circulating blood volume).<sup>31</sup> The blood samples were centrifuged and plasma was stored at -80°C until analysis.

## Midazolam

Midazolam for therapeutic infusion was manufactured and compounded by the Pharmacy A15 (Gorinchem, NL) under Good Manufacturing Practice (GMP) conditions. [ $^{14}\text{C}$ ]midazolam was synthesized by Selcia Ltd, United Kingdom at a specific activity of 1033 MBq/mmol (equal to 2.85 MBq/mg). The chemical name is 8-chloro-6-(2-fluorophenyl)-1-methyl- $^4\text{H}$ -[1- $^{14}\text{C}$ ]imidazo[1,5-a][1,4]benzodiazepine hydrochloride and it was brought in ethanol solution (96%). In the department of Radiology and Nuclear Medicine at the VU University Medical Center (Amsterdam, NL), the solution was further diluted to the required concentration with sodium chloride 0.9% solution (Fresenius Kabi, Zeist, NL) under GMP conditions. The final [ $^{14}\text{C}$ ]midazolam concentration was 210-270 Bq/mL with 1 Bq=0.31 ng [ $^{14}\text{C}$ ]midazolam.

## Measurements

### *[ $^{14}\text{C}$ ]midazolam, [ $^{14}\text{C}$ ]OHM and [ $^{14}\text{C}$ ]OHMG plasma concentration quantification*

#### ***Plasma sample extraction and Ultra Performance Liquid Chromatography Separation***

The Ultra Performance Liquid Chromatography (UPLC) and Accelerator Mass Spectrometry (AMS) (see 3.5.1.2) qualifications were performed in accordance with the recommendation of the European Bioanalytical Forum.<sup>32</sup> Methanol (200  $\mu\text{L}$ , containing unlabeled midazolam, OHM and OHMG) was added to 15  $\mu\text{L}$  plasma samples in order to precipitate proteins and to extract the test substance using protein precipitation plates (Phenomenex). Each run consisted of samples and eight calibrator levels (180, 60, 20, 10, 5, 2.5, 1.25 and 0.625 Bq/L) in duplicate, plus three different QC levels (135, 7.5 and 0.625 Bq/L) in duplicate to quantify midazolam, OHM and OHMG. 30  $\mu\text{L}$  extract was evaporated to dryness, re-dissolved in 30  $\mu\text{L}$  1 mM ammonium formate in water + 5% AcN and 25  $\mu\text{L}$  was injected on the UPLC. The fractions where midazolam, OHM and OHMG eluted from the column were collected for each sample, transferred to a tin foil cup, evaporated to dryness and analyzed using Combustion- $\text{CO}_2$ -AMS. Each series was accompanied by 2 calibrations lines at eight levels, and QCs in triplicate at three levels. Accuracy and precision complied with the EBF criteria of 20% of 2/3 of the QCs.

### **Accelerator Mass Spectrometry analysis**

[<sup>14</sup>C]levels were quantified as described before.<sup>16, 33</sup> The tin foil cups (see 5.5.1.1) were combusted on an elemental analyser (Vario Micro; Elementar, Langenselbold, Germany). Generated CO<sub>2</sub> was transferred to an in-house developed gas interface, composed of a zeolite trap and syringe.<sup>33</sup> CO<sub>2</sub> was adsorbed to the trap on the interface; after heating of the trap, the CO<sub>2</sub> was transferred to a vacuum syringe using helium. A final CO<sub>2</sub>/helium mixture of 6% was directed to the AMS ion source, at a pressure of 1 bar and a flow of 60 µL min<sup>-1</sup>. A 1-MV Tandetron AMS (High Voltage Engineering Europe B.V., Amersfoort, the Netherlands)<sup>34</sup> was used. The lower limit of quantification (LLOQ) of the LC-AMS was 0.31 Bq/L and the upper limit was 200 Bq/L.

### **Therapeutic midazolam plasma concentration quantification by liquid chromatography–tandem mass spectroscopy**

Midazolam and the major metabolites were quantified by means of a liquid chromatography–tandem mass spectroscopy (LC-MS/MS) with electrospray ionization in the positive ionization mode (Waters) validated according to Food and Drug Administration (FDA) guidance.<sup>35</sup> The LLOQ for midazolam was 2 µg/L, for OHM 3 µg/L and for OHMG 10 µg/L. The upper limit of quantification for midazolam was 2400 µg/L, for OHM 2300 µg/L and for OHMG 3000 µg/L. The internal standard is midazolam-d4. During analysis 3 standards (covering the whole range of linearity) and 4 quality controls are used from different manufacturers, to obtain objectivity. 100 µL sample is used. After sample preparation (e.g. adding internal standard), the supernatant (3 µL) is injected in the system. The runtime is 7.6 minutes per sample.

### **Data collection**

We collected data on the doses of therapeutic midazolam and [<sup>14</sup>C]midazolam and the respective timings of administration and blood sampling. Patient characteristics and relevant clinical and laboratory measurements were prospectively recorded.

### **Pharmacokinetic analysis**

#### **Population pharmacokinetics to assess the oral bioavailability**

The oral bioavailability of a drug was quantified by means of a population PK analysis. All [<sup>14</sup>C]midazolam and midazolam concentration–time data were analyzed simultaneously using nonlinear mixed effects modeling with NONMEM version 7.4 (ICON; Globomax LLC, Ellicott, MD) after log transformation of the concentration data. [<sup>14</sup>C]midazolam concentrations under the AMS detection limit (<LLOQ) were discarded.<sup>36</sup> Pirana 2.9.7, R (version 3.4.1), and R-studio (version 1.0.153) were used to visualize the data. Model development was in four steps (see Methods S1 for detailed information): (1) selection of a structural model, (2) selection of an error model, (3) covariate analysis, and (4)

internal validation of the model. The absorption rate constant ( $k_a$ ) for midazolam was fixed at  $4.16 \text{ h}^{-1}$ , which yields peak concentrations to be reached round 30 min, which is in agreement with the observed  $t_{\max}$  in our data and with values reported for children in previous literature.<sup>13</sup>

### ***Non-compartmental analysis to assess the systemic exposure to midazolam and its major metabolites after oral dosing***

To calculate the systemic exposure of midazolam and its major metabolites, the concentration-time areas under the curve after oral dosing were determined with non-compartmental analyses. The [ $^{14}\text{C}$ ]midazolam and metabolite concentrations were measured in Bq/L. Values were converted from Bq to ng based on molecular weights ( $9.6 \cdot 10^{-4} \text{ mol/Bq}$ ), where [ $^{14}\text{C}$ ]midazolam was 325.8 g/mol (0.31 ng/Bq), [ $^{14}\text{C}$ ]OHM 341.8 g/mol (0.33 ng/Bq) and [ $^{14}\text{C}$ ]OHMG 517.9 g/mol (0.50 ng/Bq). The AUC from time zero to the last sampling time point ( $\text{AUC}_{0-\text{tlast}}$ ) was calculated using the log-linear trapezoidal method; the AUC from time zero to infinite time ( $\text{AUC}_{0-\text{inf}}$ ) was calculated by extrapolation beyond the last observation.<sup>37</sup> If  $\text{AUC}_{\text{tlast}-\text{inf}}$  was larger than 20% of the actual  $\text{AUC}_{0-\text{tlast}}$ , then the  $\text{AUC}_{0-\text{inf}}$  was excluded from the analysis, as it would limit the accuracy of the results and hence would introduce unreliable estimation of the  $\text{AUC}_{0-\text{inf}}$ . The first sample below the LLOQ was set on 0.155 Bq/L ( $0.5 \cdot \text{LLOQ}$ ), and any following samples  $< \text{LLOQ}$  were discarded.

The ratios  $\text{AUC}_{0-\text{tlast}} [\text{C}]^{14}\text{OHM} / [\text{C}]^{14}\text{midazolam}$  (OHM/M) and ratio  $\text{AUC}_{0-\text{tlast}} [\text{C}]^{14}\text{OHM} / [\text{C}]^{14}\text{OHMG}$  (OHM/OHMG) were calculated with  $\text{AUC}_{0-\text{tlast}}$  in Bq/L/h and therefore correction of molecular weight was not necessary. All PK parameters derived from individual patients were estimated using the Excel PKsolver add-in software.<sup>37</sup>

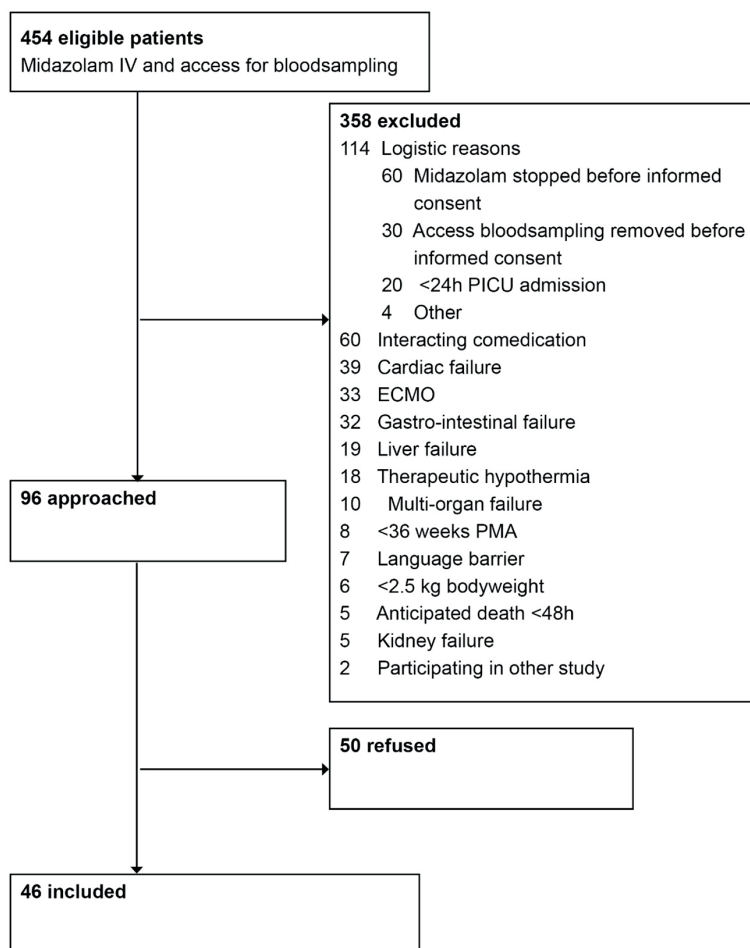
The relationships between AUC and AUC ratios and postnatal age were described with Nonparametric Spearman's rank correlation. All statistical tests were two-sided and a significance level of  $p=0.05$  was used.

## **RESULTS**

### **Population**

Between October 2015 and March 2018, ninety-six of 454 screened patients were eligible to participate, and informed consent was obtained from parents of 46 of these children (median gestational age at birth of 39.0 [29.4 – 43.0] weeks and a median postnatal age of 9.8 weeks [2 days – 5.3 years]) (see Figure 1). Three-quarters were 0-6 months old. Table 1 provides the characteristics of these 46 children.



**Figure 1** Flowchart of patient recruitment

Data of three of these 46 children were excluded from further analysis. In one, extubated shortly after receiving the [ $^{14}\text{C}$ ]midazolam microtracer, no [ $^{14}\text{C}$ ]midazolam concentration could be detected in the plasma samples. The undetectable concentrations can be explained by clinical practice, because immediately before extubation the child's stomach is completely emptied to avoid aspiration. The two others had, in hindsight, received interacting co-medication that induced CYP3A.

### Oral bioavailability

In the final population PK model, the typical oral bioavailability in the population was 66% with a high IIV of 0.86; individual bioavailability estimates ranged from 25% to 85%. See Figure 2 for the variability in individual bioavailability. All PK parameter estimates of this model are presented in Table 2.

**Table 1** Characteristics of patients included in the analysis presented as median (range) or number

Patient characteristics		
Number of patients (n)	46	
Location (n Erasmus MC/n Radboudumc)	39/7	
Postnatal age (weeks)	9.8 (0.3 – 276.4)	
Postmenstrual age (weeks)	48.9 (38.9 – 316.4)	
Weight (kg)	4.7 (2.8 – 18.0)	
Z-score weight for age*	-0.9 (-3.0 – 2.5)	
Gender (M/F)	29/17	
Ethnicity (Caucasian/other)	41/5	
Reason for admission (n)	Respiratory failure	
	• Pneumonia/bronchiolitis	18
	• Congenital cardiac abnormality	7
	• Pulmonary hypertension	2
	• Traumatic injury to the airways	2
	• Lobar emphysema	2
	• Meconium aspiration	1
	Post cardiac surgery	12
	Status epilepticus	2
Disease severity scores		
PELOD	11 (0-21)	
Number of organs failing on study day	1 (0 – 2)	
PRISM	16 (3 – 32)	
PIM	-2.5 (-4.8 – -0.4)	
Laboratory values at day of administration [ <sup>14</sup> C]midazolam		
Plasma creatinine (μmol/L)	29 (11 – 63)	
ASAT (U/L)	42 (16 – 155)	
ALAT (U/L)	18 (6 – 138)	
CRP (mg/L)	43 (2 – 298)	
Study medication		
Dose [ <sup>14</sup> C]midazolam (Bq)	282.7 (165.0 – 1080.0)	
Dose [ <sup>14</sup> C]midazolam (ng)	87.6 (51.15 – 334.8)	

PELOD=Pediatric Logistic Organ Dysfunction; PRISM=Pediatric Risk of Mortality; PIM=Pediatric Index of Mortality; ASAT= aspartate-aminotransferase; ALAT=alanine-aminotransferase; CRP=C-reactive protein; \*As determined by TNO growth curves

For this model, a total of 30 [<sup>14</sup>C]midazolam concentrations under the AMS detection limit (<LLOQ) were discarded.<sup>36</sup> The complete dataset included 326 and 245 radiolabeled and cold midazolam concentrations, respectively, from 43 patients. The final model entails a one-compartment model that best described the PK of oral and IV midazolam. Inclusion of IIV for clearance, volume of distribution, and oral bioavailability improved the model

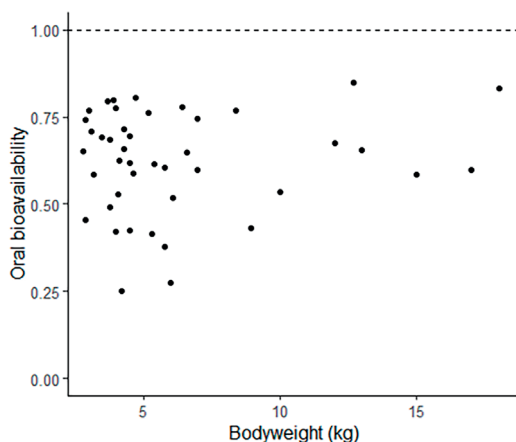


**Figure 2** Oral bioavailability of midazolam and its variability versus bodyweight. Bodyweight did not explain the variability in oral bioavailability.

statistically significantly. Bodyweight was the most significant predictor for clearance ( $\Delta\text{OFV} -11.11$ ) and volume of distribution ( $\Delta\text{OFV} -15.95$ ) in exponential relationships (see Table 2). After this inclusion, both the variance of the IIV for clearance and volume of distribution decreased. Age and other tested covariates were found not statistically significant after inclusion of bodyweight.

All relative standard error (RSE) values of the parameter estimates were below 50%, indicating that the estimates could be obtained from the data with good precision. The diagnostic plots for the final model are presented in Figure S1 (oral data) and in Figure S2 (IV data). Both figures indicate that the model describes the obtained data accurately, upon both oral and IV administration, even though for the oral data more random variability is observed. The robustness of the estimated model parameters was evaluated in a bootstrap analysis. The bootstrap analysis confirmed the precision of parameter estimates of the final model, as the parameter estimates were very similar to the bootstrap medians and within the 95% confidence interval (Table 2). The distribution of the NPDEs indicates that the model can adequately predict both the median trend and the variability in the observed concentrations. This is further supported by the absence of visible trends in NPDE versus time and NPDE versus predictions (see Figure S3 and S4).

### Systemic exposure to midazolam and its major metabolites after oral dosing

The systemic exposures, as reflected by the AUCs of midazolam and its major metabolites after administration of the oral [ $^{14}\text{C}$ ]midazolam microtracer are presented in Table 3. The complete dataset included data on 335 plasma samples from 43 patients. A total of 21 (6%), 41 (12%), and 14 (4%) samples were set on 0.5\*LLOQ for respectively [ $^{14}\text{C}$ ]midazolam, [ $^{14}\text{C}$ ]OHM and [ $^{14}\text{C}$ ]OHMG. A total of 9 (3%), 93 (28%), and 2 (0.6%) samples were discarded for respectively [ $^{14}\text{C}$ ]midazolam, [ $^{14}\text{C}$ ]OHM and [ $^{14}\text{C}$ ]OHMG. Eight (19%),

**Table 2** Parameter estimates of a one-compartmental model.

Parameter	Model parameters estimates (RSE%)	Bootstrap median (2.5 <sup>th</sup> to 97.5 <sup>th</sup> bootstrap percentile)
<b>Oral bioavailability</b>		
	$F_i = e^{\log(TVF/(1-TVF))} / (1 + e^{\log(TVF/(1-TVF))})$	
TVF	0.66 (8%)	0.66 (0.56-0.78)
<b>Absorption rate constant</b>		
ka (h <sup>-1</sup> )	4.16 FIXED	-
<b>Clearance</b>		
	$CL_i = CL_{5kg} * (WT/5)^{k1}$	
CL <sub>5kg</sub> (L/h)	0.98 (13%)	0.99 (0.78-1.28)
k1	0.92 (31%)	0.93 (0.44-1.59)
<b>Volume of distribution</b>		
	$V_i = V_{5kg} * (WT/5)^{k2}$	
V <sub>5kg</sub> (L)	8.70 (11%)	8.68 (6.94-10.78)
k2	1.16 (21%)	1.17 (0.79-1.85)
<b>Inter-individual variability</b>		
ω <sup>2</sup> CL	0.65 (19%)	0.61 (0.39-0.87)
ω <sup>2</sup> V	0.40 (24%)	0.37 (0.18-0.58)
ω <sup>2</sup> TVF	0.86 (49%)	0.78 (0.17-1.78)
<b>Residual error</b>		
Additive error oral [ <sup>14</sup> C]midazolam data	0.08 (29%)	0.07 (0.04-0.13)
Additive error IV midazolam data	0.47 (30%)	0.47 (0.25-0.77)

ω<sup>2</sup> = variance for the inter-individual variability of the indicated parameter; CL = clearance; CL<sub>i</sub> = predicted clearance of individual i; CL<sub>5kg</sub> = population-predicted clearance for a subject with a median weight of 5 kg; CV = coefficient of variation; F = absolute oral bioavailability; F<sub>i</sub> = predicted absolute oral bioavailability of individual i; k1 = exponent to relate body weight to clearance; k2 = exponent to relate body weight to volume of distribution; RSE = relative standard error; TVF = population parameter in the logit equation for oral bioavailability; V = volume of distribution; V<sub>i</sub> = individual predicted volume of distribution for individual i; V<sub>5kg</sub> = population-predicted volume for a subject with a median weight of 5 kg; WT = body weight

**Table 3** Area under the curves of midazolam and its major metabolites 1-OH-midazolam and 1-OH-midazolam-glucuronide and their ratios after administration of an oral [<sup>14</sup>C]midazolam microtracer (20.3 [14.1-23.6] ng/kg; 58 [40-67] Bq/kg)

		Midazolam	OHM	OHMG
AUC <sub>0-tlast</sub>	Bq/L/h	162.6 (10.4-898.4) (n=43)	12.0 (1.1-77.0) (n=38)	254.4 (62.6-821.6) (n=43)
	ng/L/h	50.4 (3.2-278.5) (n=43)	4.0 (0.4-25.4) (n=38)	127.2 (31.3-410.8) (n=43)
AUC <sub>0-inf</sub>	Bq/L/h	160.9 (10.6-753.3) (n=32)	17.9 (3.0-81.7) (n=29)	272.2 (71.6-921.8) (n=22)
	ng/L/h	49.9 (3.3-233.5) (n=32)	5.9 (1.0-27.0) (n=29)	136.1 (35.8-460.9) (n=22)
AUC <sub>0-tlast</sub> ratio OHM/M			0.1 (<0.1-1.5) (n=38)	
AUC <sub>0-tlast</sub> ratio OHM/OHMG			0.05 (<0.01 – 0.20) (n=38)	

Data is presented as median (range). n = number of patients. M = midazolam, OHM = 1-OH-midazolam, OHMG = 1-OH-midazolam-glucuronide, AUC = Area Under the Curve. See 4.3 for explanation on the patient numbers.

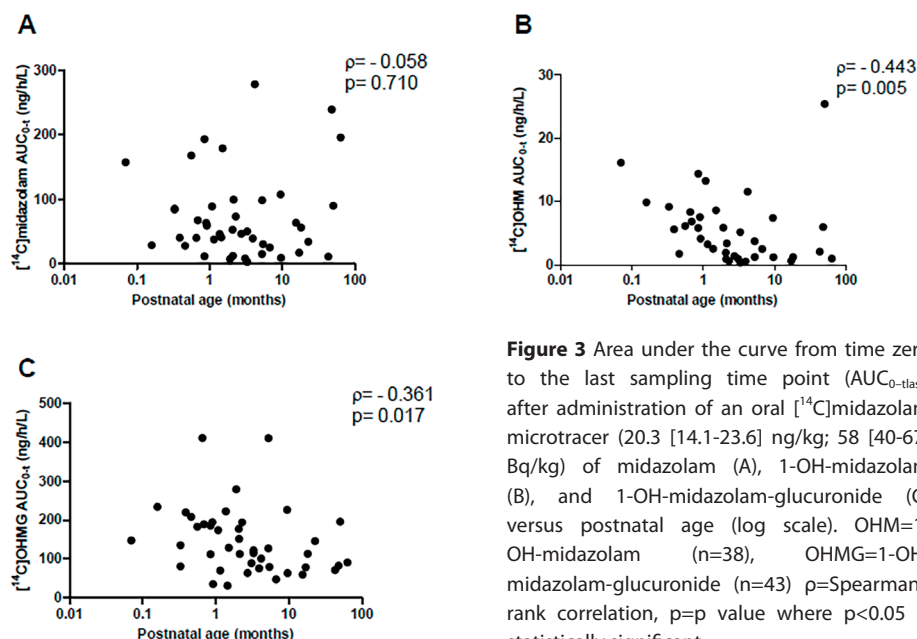


**Figure 3** Area under the curve from time zero to the last sampling time point ( $\text{AUC}_{0-\text{tlast}}$ ) after administration of an oral  $^{14}\text{C}$ midazolam microtracer (20.3 [14.1-23.6] ng/kg; 58 [40-67] Bq/kg) of midazolam (A), 1-OH-midazolam (B), and 1-OH-midazolam-glucuronide (C) versus postnatal age (log scale). OHM=1-OH-midazolam (n=38), OHMG=1-OH-midazolam-glucuronide (n=43)  $\rho$ =Spearman's rank correlation,  $p$ =p value where  $p < 0.05$  is statistically significant

9 (21%), and 21 (49%) patients were excluded from  $\text{AUC}_{0-\text{inf}}$  analyses of respectively  $^{14}\text{C}$ midazolam,  $^{14}\text{C}$ OHM and  $^{14}\text{C}$ OHMG as the  $\text{AUC}_{\text{tlast}-\text{inf}}$  was larger than 20% of the actual  $\text{AUC}_{0-\text{tlast}}$ . For another 3 patients (7%) the  $\text{AUC}_{0-\text{inf}}$  of  $^{14}\text{C}$ midazolam could not be calculated. For 2 patients, only one plasma sample taken after the absorption phase was available due to loss of the arterial catheter, and in one patient the plasma concentration-time profile had no apparent log-linear slope, for which no explanation was found. For 5 patients (12%) the  $\text{AUC}_{0-\text{tlast}}$  and  $\text{AUC}_{0-\text{inf}}$  of OHM could not be calculated as most plasma concentrations were  $< \text{LLOQ}$ .

Figure 3 shows the  $\text{AUC}_{0-\text{tlast}}$  of  $^{14}\text{C}$ midazolam,  $^{14}\text{C}$ OHM, and  $^{14}\text{C}$ OHMG versus postnatal age after administration of the oral  $^{14}\text{C}$ midazolam microtracer. The AUC of  $^{14}\text{C}$ OHM and  $^{14}\text{C}$ OHMG were the highest for the youngest age groups, even though the AUC of  $^{14}\text{C}$ midazolam was similar across age. Analysis of the data revealed a statistically significant negative correlation for both  $^{14}\text{C}$ OHM  $\text{AUC}_{0-\text{tlast}}$  and  $\text{AUC}_{0-\text{inf}}$  and  $^{14}\text{C}$ OHMG  $\text{AUC}_{0-\text{tlast}}$  and  $\text{AUC}_{0-\text{inf}}$  with postnatal age (see Figure 3B and C for  $\text{AUC}_{0-\text{tlast}}$ , results for  $\text{AUC}_{0-\text{inf}}$  not shown). No significant relationship was identified between postnatal age and  $^{14}\text{C}$ midazolam  $\text{AUC}_{0-\text{tlast}}$  (see Figure 3),  $^{14}\text{C}$ midazolam  $\text{AUC}_{0-\text{inf}}$ , OHM/M AUC ratio, and OHM/OHMG ratio (data not shown).

## DISCUSSION

To study the oral bioavailability of midazolam and the systemic exposure to midazolam and its major metabolites in children, we designed a prospective oral [ $^{14}\text{C}$ ]midazolam microtracer population PK study in children receiving midazolam for clinical purposes. Our main observations were that (1) the median oral bioavailability of midazolam was 66% and varied greatly with a range of 25-85% and (2) the systemic exposure (AUC) of the major metabolites 1-OHM formed by CYP3A and 1-OHMG formed out of 1-OHM by UGT2B4, -2B7 and -1A4 were highest for the youngest age ranges, despite weight normalized midazolam doses.

Our study design has previously been applied to investigate the oral bioavailability of paracetamol and the systemic exposure to its metabolites in children<sup>15, 17</sup> and has now shown to be successful for midazolam. The informed consent rate of 50% was in agreement with the consent rate of other non-therapeutic studies in pediatric intensive care. Moreover, our population PK model results were in agreement with reported values on oral PK parameters for midazolam, confirming the feasibility of the [ $^{14}\text{C}$ ]midazolam microtracer approach. The median CL of 0.20 L/h/kg in our study was in line with literature values of 0.26 L/h/kg in children 0-18 year in the IC.<sup>38</sup> Our median V of 1.7 L/kg lies in the range of 0.2-3.5 L/kg as found in critically ill children with an age between 8 days and 16 years.<sup>39</sup>

More specifically, for the oral bioavailability in our patients, of whom three-quarters were 0-6 months old, the median of 66% is lower than the reported median value of 92% (range 67 to 95%) in 37 preterm neonates with a gestational age of 26-34 weeks<sup>11</sup> and higher than the reported median value of 21% (range 2 to 78%) in 264 older children of 1-18 years.<sup>12</sup> Also the reported mean  $\pm$ SD of  $28 \pm 7\%$  in adults is lower than in our population.<sup>40</sup> These latter findings can be explained by the expected CYP3A ontogeny, as older children and adults are thought to have a higher CYP3A activity in both the gut wall and liver, resulting in a lower oral bioavailability<sup>3</sup> than found in our patients, and *vice versa* for preterm neonates. Statistically significant covariate relationships that could explain part of the inter-individual variability in oral bioavailability were not found. However, a highly variable oral bioavailability was also found in previous pediatric PK studies<sup>10-12</sup>, particularly in preterm neonates<sup>10, 11</sup>, and we can conclude it is independent of the microtracer-design. The higher variability in oral bioavailability in our study may be due to the nature of the studied population: stable, critically ill patients instead of healthier patients. A previous study from *Vet et al.* found a significant impact of organ failure on midazolam clearance<sup>38</sup>, with the greatest impact on midazolam clearance in the presence of  $\geq 3$  failing organs and inflammation as reflected by CRP.<sup>38</sup> We were

not able to identify these covariates in our data, likely because children with severe circulatory, kidney or liver failure were excluded, and the number of failing organs in our study ranged from 0 to 3 per child. CRP values in our study were comparable to those in the previous study from *Vet et al.*; i.e., (median [range] 43 [2 – 298] vs 32 [0.3–385] mg/L, resp.). However, we only included 6 patients with a CRP > 100 mg/L, whereas the previously reported cohort consisted of more patients with CRP > 100 mg/L.

The variability in oral bioavailability as observed in our study leads to unpredictable systemic exposure to midazolam, and potentially also other CYP3A-substrates, after oral dosing in (critically ill) children. These children may be at risk of subtherapeutic or toxic exposure after oral dosing of other CYP3A-substrates.

In addition, the systemic exposures of the main metabolites OHM and OHMG were highest in the youngest age ranges at similar exposure of midazolam across age. This observation can most likely not be attributed solely to CYP3A ontogeny, but to other developmental changes as well, as the exposure of each metabolite is dependent on various factors. First, the CYP3A activity drives the formation of 1-OHM. Second, the reported age-related changes in UGTs may increase the glucuronidation of 1-OHM over age.<sup>41</sup> The age-related decrease in AUC of 1-OHMG can be partly explained by the fact that the OHMG metabolite is excreted renally and considering that children's renal function increases over age<sup>42-44</sup> This explanation is supported by a reported postconceptional age-related increase in urinary excretion of OHMG in preterm neonates.<sup>45</sup> A metabolic shift, as seen for paracetamol where a switch from mainly sulphation to glucuronidation is seen in the first of years life is less likely. As in the case of midazolam this would mean decreased formation of another metabolite than 1-OHMG in the younger age group compared to older children than adults. But as no other major metabolite for midazolam, in addition the minor metabolites 4-OHM(G) and MG have been identified in adults, this seems unlikely.<sup>46, 47</sup> Third, the distribution volume of the metabolites may change with age, impacting the total systemic exposure of the metabolites.<sup>48</sup> Considering the case-reports on the association between OHMG accumulation and prolonged sedation<sup>25</sup>, clinicians should be aware that the systemic exposure to OHMG may be higher in neonates than in older children, potentially also contributing to its sedative effect.

The following limitations of the study need to be addressed. First, our innovative study design limits the inclusion of pharmacodynamic (PD) data as the extremely low dose of the microtracer midazolam is not expected to have pharmacological effects. Hence, we can speculate that the variability in oral availability of midazolam and the higher systemic exposure to OHMG may lead to subtherapeutic or toxic exposure. The real impact of this variability on pharmacodynamics parameters should be assessed in future studies.

Second, data of 21 patients were excluded from  $AUC_{0-inf}$  analyses of OHMG because the elimination of this metabolite was not complete after 24h. In retrospect, longer sampling time would have benefited this analysis. Third, the absorption of midazolam may be influenced by food intake as food in the gastrointestinal tract may alter the gastrointestinal physiology, including the motility patterns, intestinal transit time, and the local blood flow.<sup>49</sup> However, information on food was not collected and the study was not powered to detect an effect of food on midazolam absorption but may have contributed to the variability in our data. Also, dose linearity of the PK of an oral microdose to those of a therapeutic dose of midazolam has been established in adults.<sup>50-52</sup> We made the assumption that this also accounts for children, further supported by dose-linearity of IV midazolam in children<sup>53</sup>, but not been formally established.

This study presents some future opportunities. Recently, a framework was published for between-drug extrapolation of covariate models<sup>54</sup> which was used by *Brussee et al* to study whether scaling with a pediatric covariate function from midazolam will lead to accurate clearance values of other CYP3A-substrates.<sup>55</sup> Clearances of drugs were accurately scaled when they were mainly eliminated by CYP3A-mediated metabolism with, for example, high protein binding to albumine (> 90%) and a low-to-intermediate extraction ratio of <0.55 in adults. However, the covariate relationship for clearance was based on data from children >1 year of age. As our population consists of infants mainly <1 years of age, our data now present a unique opportunity to test the proposed framework for this younger age group. Also, this study design is promising for drugs under development. When there is interest to, besides an IV administration, study the drug as an oral administration, an oral [<sup>14</sup>C] labelled microtracer can be added without setting up a new pediatric cohort, or *vice versa*. Lastly, a microdose pediatric study can be used to obtain information on the PK for drugs with high toxicity, like oncology agents, and clear PK/PD relationship followed by the determination of an effective dose based on the PK profile.

In conclusion, the results of this population PK study added data on oral bioavailability of midazolam as a marker for CYP3A in an age range where data was missing. It shows that children may be at an increased risk of subtherapeutic or toxic exposure of midazolam and potentially also of other CYP3A-substrates when dosed orally. The study design with an oral [<sup>14</sup>C]microtracer was shown successful for safely studying the oral bioavailability of midazolam in children. To ultimately improve the safety and efficacy of pediatric drug therapy, we recommend to consider study designs with microdoses for minimal risk PK studies and [<sup>14</sup>C]microtracer studies to elucidate oral bioavailability.



## REFERENCES

1. Notterman, D.A. Sedation with intravenous midazolam in the pediatric intensive care unit. *Clin Pediatr (Phila)* 1997;36(8):449-54.
2. Liacouras, C.A., Mascarenhas, M., Poon, C. & Wenner, W.J. Placebo-controlled trial assessing the use of oral midazolam as a premedication to conscious sedation for pediatric endoscopy. *Gastrointest Endosc* 1998;47(6):455-60.
3. de Wildt, S.N., Kearns, G.L., Leeder, J.S. & van den Anker, J.N. Cytochrome P450 3A: ontogeny and drug disposition. *Clin Pharmacokinet* 1999;37(6):485-505.
4. Williams, J.A. et al. Comparative metabolic capabilities of CYP3A4, CYP3A5, and CYP3A7. *Drug Metab Dispos* 2002;30(8):883-91.
5. Stevens, J.C. et al. Developmental expression of the major human hepatic CYP3A enzymes. *J Pharmacol Exp Ther* 2003;307(2):573-82.
6. Fakhoury, M. et al. Localization and mRNA expression of CYP3A and P-glycoprotein in human duodenum as a function of age. *Drug Metab Dispos* 2005;33(11):1603-7.
7. Johnson, T.N., Tanner, M.S., Taylor, C.J. & Tucker, G.T. Enterocytic CYP3A4 in a paediatric population: developmental changes and the effect of coeliac disease and cystic fibrosis. *Br J Clin Pharmacol* 2001;51(5):451-60.
8. Streetman, D.S., Bertino, J.S., Jr. & Nafziger, A.N. Phenotyping of drug-metabolizing enzymes in adults: a review of in-vivo cytochrome P450 phenotyping probes. *Pharmacogenetics* 2000;10(3):187-216.
9. de Wildt, S.N., Ito, S. & Koren, G. Challenges for drug studies in children: CYP3A phenotyping as example. *Drug Discov Today* 2009;14(1-2):6-15.
10. de Wildt, S.N., Kearns, G.L., Hop, W.C., Murry, D.J., Abdel-Rahman, S.M. & van den Anker, J.N. Pharmacokinetics and metabolism of oral midazolam in preterm infants. *Br J Clin Pharmacol* 2002;53(4):390-2.
11. Brussee, J.M. et al. First-Pass CYP3A-Mediated Metabolism of Midazolam in the Gut Wall and Liver in Preterm Neonates. *CPT Pharmacometrics Syst Pharmacol* 2018;7(6):374-83.
12. Brussee, J.M. et al. Characterization of Intestinal and Hepatic CYP3A-Mediated Metabolism of Midazolam in Children Using a Physiological Population Pharmacokinetic Modelling Approach. *Pharm Res* 2018;35(9):182.
13. Reed, M.D. et al. The single-dose pharmacokinetics of midazolam and its primary metabolite in pediatric patients after oral and intravenous administration. *J Clin Pharmacol* 2001;41(12):1359-69.
14. Payne, K., Mattheyse, F.J., Liebenberg, D. & Dawes, T. The pharmacokinetics of midazolam in paediatric patients. *Eur J Clin Pharmacol* 1989;37(3):267-72.
15. Mooij, M.G. et al. Successful Use of [<sup>14</sup>C]Paracetamol Microdosing to Elucidate Developmental Changes in Drug Metabolism. *Clin Pharmacokinet* 2017;DOI: 10.1007/s40262-017-0508-6
16. Mooij, M.G. et al. Pediatric microdose study of [(<sup>14</sup>C)]paracetamol to study drug metabolism using accelerated mass spectrometry: proof of concept. *Clin Pharmacokinet* 2014;53(11):1045-51.
17. Kleiber, N. et al. Enteral Acetaminophen Bioavailability in Pediatric Intensive Care Patients Determined With an Oral Microtracer and Pharmacokinetic Modeling to Optimize Dosing. *Crit Care Med* 2019;DOI: 10.1097/CCM.0000000000004032
18. European Medicines Agency. ICH Topic M3 (R2) Non-Clinical Safety Studies for the Conduct of Human Clinical Trials and Marketing Authorization for Pharmaceuticals. 2008;

19. Food and Drug Administration US Department of Health and Human Services Guidance for Industry Investigators and Reviewers. Exploratory IND Studies. 2006;
20. Salehpour, M., Possnert, G. & Bryhni, H. Subattomole sensitivity in biological accelerator mass spectrometry. *Anal Chem* 2008;80(10):3515-21.
21. Vuong, L.T., Blood, A.B., Vogel, J.S., Anderson, M.E. & Goldstein, B. Applications of accelerator MS in pediatric drug evaluation. *Bioanalysis* 2012;4(15):1871-82.
22. Tuk, B., van Oostenbruggen, M.F., Herben, V.M., Mandema, J.W. & Danhof, M. Characterization of the pharmacodynamic interaction between parent drug and active metabolite in vivo: midazolam and alpha-OH-midazolam. *J Pharmacol Exp Ther* 1999;289(2):1067-74.
23. Heizmann, P. & Ziegler, W.H. Excretion and metabolism of 14C-midazolam in humans following oral dosing. *Arzneimittelforschung* 1981;31(12a):2220-3.
24. Seo, K.A., Bae, S.K., Choi, Y.K., Choi, C.S., Liu, K.H. & Shin, J.G. Metabolism of 1'- and 4-hydroxymidazolam by glucuronide conjugation is largely mediated by UDP-glucuronosyltransferases 1A4, 2B4, and 2B7. *Drug Metab Dispos* 2010;38(11):2007-13.
25. Bauer, T.M. et al. Prolonged sedation due to accumulation of conjugated metabolites of midazolam. *Lancet* 1995;346(8968):145-7.
26. Johnson, T.N., Rostami-Hodjegan, A., Goddard, J.M., Tanner, M.S. & Tucker, G.T. Contribution of midazolam and its 1-hydroxy metabolite to preoperative sedation in children: a pharmacokinetic-pharmacodynamic analysis. *Br J Anaesth* 2002;89(3):428-37.
27. Salman, S. et al. A novel, palatable paediatric oral formulation of midazolam: pharmacokinetics, tolerability, efficacy and safety. *Anaesthesia* 2018;73(12):1469-77.
28. RIVM. Stralingsbelasting in Nederland. <https://www.rivm.nl/stralingsbelasting-in-nederland> (2013). Accessed 10 April, 2019.
29. International Commission on Radiological Protection. 1990 Recommendations of the International Commission on Radiological Protection. *Ann ICRP* 1991;21(1-3):1-201.
30. Indiana University. Drug Interactions Flockhart Table. <https://drug-interactions.medicine.iu.edu/Main-Table.aspx>. Accessed 10 April, 2019.
31. EMA. Guideline on the investigation of medicinal products in the term and preterm neonate. (EMA/PDCO/362462/2016).
32. Highton, D., Young, G., Timmerman, P., Abbott, R., Knutsson, M. & Svensson, L.D. European Bioanalysis Forum recommendation: scientific validation of quantification by accelerator mass spectrometry. *Bioanalysis* 2012;4(22):2669-79.
33. van Duijn, E., Sandman, H., Grossouw, D., Mocking, J.A., Coulier, L. & Vaes, W.H. Automated combustion accelerator mass spectrometry for the analysis of biomedical samples in the low attomole range. *Anal Chem* 2014;86(15):7635-41.
34. Klein, M.V., Vaes, W.H.J., Fabriek, B., Sandman, H., Mous, D.J.W. & Gottdang, A.T. The 1 MV multi-element AMS system for biomedical applications at the Netherlands Organization for Applied Scientific Research (TNO). *Nucl Instr Meth Phys Res B* 2013;294(14-7).
35. Food and Drug Administration. Guidance for Industry: Bioanalytical Methods Validation. . 2001;
36. Ahn, J.E., Karlsson, M.O., Dunne, A. & Ludden, T.M. Likelihood based approaches to handling data below the quantification limit using NONMEM VI. *J Pharmacokinet Pharmacodyn* 2008;35(4):401-21.
37. Zhang, Y., Huo, M., Zhou, J. & Xie, S. PKSolver: An add-in program for pharmacokinetic and pharmacodynamic data analysis in Microsoft Excel. *Comput Methods Programs Biomed* 2010;99(3):306-14.

38. Vet, N.J. et al. Inflammation and organ failure severely affect midazolam clearance in critically ill children. *Am J Respir Crit Care Med* 2016;194(1):58-66.
39. Nahara, M.C., McMorrow, J., Jones, P.R., Anglin, D. & Rosenberg, R. Pharmacokinetics of midazolam in critically ill pediatric patients. *Eur J Drug Metab Pharmacokinet* 2000;25(3-4):219-21.
40. Brill, M.J. et al. Midazolam pharmacokinetics in morbidly obese patients following semi-simultaneous oral and intravenous administration: a comparison with healthy volunteers. *Clin Pharmacokinet* 2014;53(10):931-41.
41. Rowland, A., Miners, J.O. & Mackenzie, P.I. The UDP-glucuronosyltransferases: their role in drug metabolism and detoxification. *Int J Biochem Cell Biol* 2013;45(6):1121-32.
42. Rhodin, M.M. et al. Human renal function maturation: a quantitative description using weight and postmenstrual age. *Pediatr Nephrol* 2009;24(1):67-76.
43. Faa, G. et al. Morphogenesis and molecular mechanisms involved in human kidney development. *J Cell Physiol* 2012;227(3):1257-68.
44. Heizmann, P., Eckert, M. & Ziegler, W.H. Pharmacokinetics and bioavailability of midazolam in man. *Br J Clin Pharmacol* 1983;16 Suppl 1(43S-9S).
45. de Wildt, S.N., Kearns, G.L., Murry, D.J., Koren, G. & van den Anker, J.N. Ontogeny of midazolam glucuronidation in preterm infants. *Eur J Clin Pharmacol* 2010;66(2):165-70.
46. Klieber, S. et al. Contribution of the N-glucuronidation pathway to the overall in vitro metabolic clearance of midazolam in humans. *Drug Metab Dispos* 2008;36(5):851-62.
47. Hyland, R. et al. In vitro and in vivo glucuronidation of midazolam in humans. *Br J Clin Pharmacol* 2009;67(4):445-54.
48. Kearns, G.L., Abdel-Rahman, S.M., Alander, S.W., Blowey, D.L., Leeder, J.S. & Kauffman, R.E. Developmental pharmacology--drug disposition, action, and therapy in infants and children. *N Engl J Med* 2003;349(12):1157-67.
49. Abuhelwa, A.Y., Williams, D.B., Upton, R.N. & Foster, D.J. Food, gastrointestinal pH, and models of oral drug absorption. *Eur J Pharm Biopharm* 2017;112(234-48).
50. Lappin, G. et al. Use of microdosing to predict pharmacokinetics at the therapeutic dose: experience with 5 drugs. *Clin Pharmacol Ther* 2006;80(3):203-15.
51. Hohmann, N., Kocheise, F., Carls, A., Burhenne, J., Haefeli, W.E. & Mikus, G. Midazolam microdose to determine systemic and pre-systemic metabolic CYP3A activity in humans. *Br J Clin Pharmacol* 2015;79(2):278-85.
52. Halama, B., Hohmann, N., Burhenne, J., Weiss, J., Mikus, G. & Haefeli, W.E. A nanogram dose of the CYP3A probe substrate midazolam to evaluate drug interactions. *Clin Pharmacol Ther* 2013;93(6):564-71.
53. van Groen, B.D. et al. Dose-linearity of the pharmacokinetics of an intravenous [(14) C]midazolam microdose in children. *Br J Clin Pharmacol* 2019;10.1111/bcp.14047
54. Calvier, E.A.M. et al. Drugs Being Eliminated via the Same Pathway Will Not Always Require Similar Pediatric Dose Adjustments. *CPT Pharmacometrics Syst Pharmacol* 2018;7(3):175-85.
55. Brussee, J.M. et al. A Pediatric Covariate Function for CYP3A-Mediated Midazolam Clearance Can Scale Clearance of Selected CYP3A Substrates in Children. *AAPS J* 2019;21(5):81.
56. Mould, D.R. & Upton, R.N. Basic concepts in population modeling, simulation, and model-based drug development. *CPT Pharmacometrics Syst Pharmacol* 2012;1(e6).
57. Ince, I., Knibbe, C.A., Danhof, M. & de Wildt, S.N. Developmental changes in the expression and function of cytochrome P450 3A isoforms: evidence from in vitro and in vivo investigations. *Clin Pharmacokinet* 2013;52(5):333-45.

58. Krekels, E.H. et al. From Pediatric Covariate Model to Semiphysiological Function for Maturation: Part II-Sensitivity to Physiological and Physicochemical Properties. CPT Pharmacometrics Syst Pharmacol 2012;1(e10).
59. Comets, E., Brendel, K. & Mentre, F. Computing normalised prediction distribution errors to evaluate nonlinear mixed-effect models: the npde add-on package for R. Comput Methods Programs Biomed 2008;90(2):154-66.

## SUPPLEMENTARY INFORMATION

**Methods S1** Population pharmacokinetic model development to assess the oral bioavailability

### Model selection

For model selection, we used the objective function value (OFV) and standard goodness of fit (GOF) plots. For the OFV, a drop of more than 3.84 points between nested models was considered statistically significant, which corresponds to  $p < 0.05$  assuming a chi-square distribution.<sup>56</sup> For the structural model, one, two, and three compartment models were tested. For the error model an additive error model in the log-domain was used. Inclusion of log-normally distributed inter-individual variability (IIV) was tested on all model parameters. For bioavailability, a logit transformation with a normal distribution for inter-individual variability was used to avoid individual bioavailability estimates outside the 0%-100% range. The absorption rate constant ( $k_a$ ) for midazolam was fixed at  $4.16 \text{ h}^{-1}$ , which yields peak concentrations to be reached round 30 min, which is in agreement with the observed  $t_{max}$  in our data and with values reported for children in previous literature.<sup>13</sup>

### Covariate analysis

The correlation with PK parameters was evaluated for the following continuous covariates: postnatal age, postmenstrual age, bodyweight, creatinine, urea, alanine aminotransferase (ALAT), aspartate aminotransferase (ASAT), alkaline phosphatase (AF), Gamma-glutamyltransferase ( $\gamma$ -GT), C-reactive protein (CRP), leukocytes count, Pediatric Risk of Mortality (PRISM) score, and Pediatric Index of Mortality (PIM) score. Categorical covariates included gender, Pediatric Logistic Organ Dysfunction (PELOD) score, and organ failure as determined by the PELOD score.

Potential covariates were evaluated using forward inclusion and backward elimination with cut-off values of  $p < 0.005$  (OFV -7.9 points) and  $p < 0.001$  (OFV -10.8 points), respectively. In addition, for a covariate to be retained in the model, its inclusion had to result in a decline in unexplained variability and/or improved goodness of fit plots.<sup>57, 58</sup>

### Model evaluation

The model was internally validated using a bootstrap analysis in Perl-speaks-NONMEM (PsN), for which five hundred datasets were resampled with replacement from the original datasets and refitted to the model. The obtained parameter values from these 500 model fits were summarized as median values and 95% confidence intervals, which were compared to the values obtained in the original model fit.

Normalized prediction distribution errors (NPDE) were calculated with the NPDE package in R.<sup>59</sup> For this method, the data set used for model development was simulated a thousand times with inclusion of inter-individual and residual variability. The distribution of obtained NPDE values in the overall dataset as well as the distribution of NPDE values versus time and predicted concentrations was assessed. The analysis was stratified for oral administration and for IV administration.

**Figure S1** Goodness-of-fit plots of the oral [ $^{14}\text{C}$ ]midazolam data for the final model. A. Log-value of observed plasma concentrations vs. log-value of population predicted concentrations. B. Log observed plasma concentrations vs. log individual predicted concentrations. C. Conditional weighted residuals (CWRES) versus log population predictions. D. CWRES versus time after dosing.

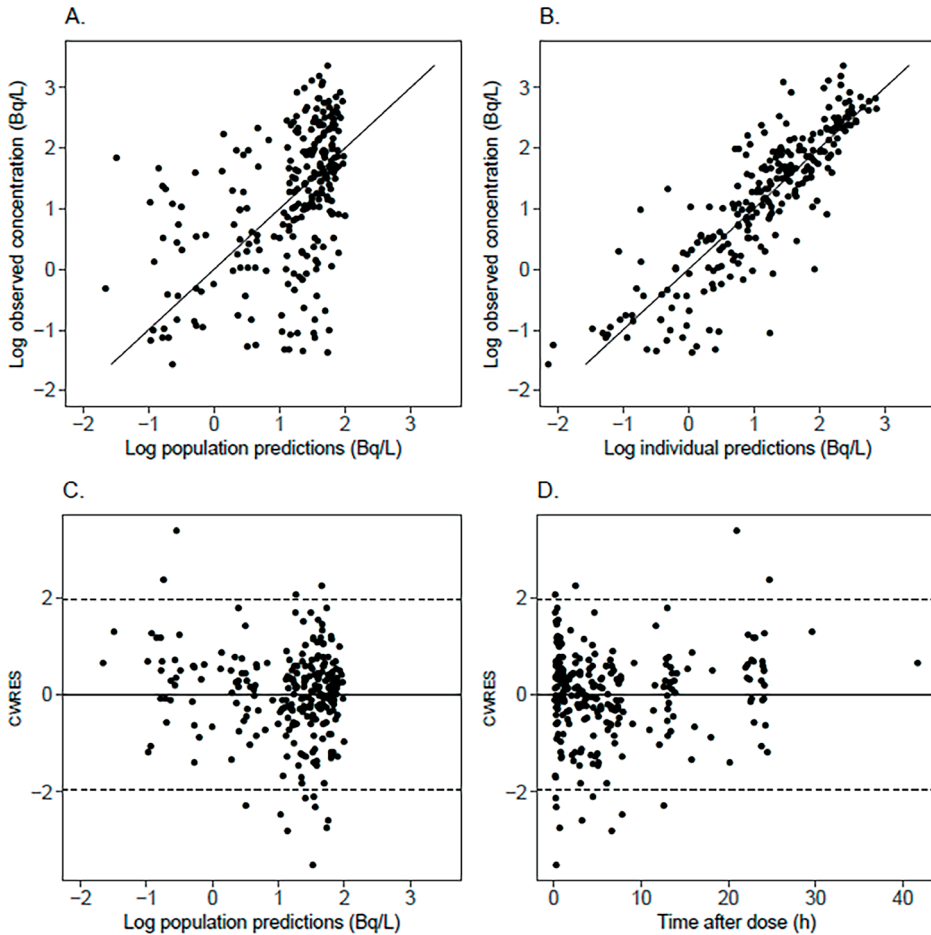


**Figure S2** Goodness-of-fit plots of the intravenous midazolam data for the final model. A. Log observed plasma concentrations vs. log population predicted concentrations. B. Log observed plasma concentrations vs. log individual predicted concentrations. C. Conditional weighted residuals (CWRES) versus log population predictions. D. CWRES versus time after first dose.

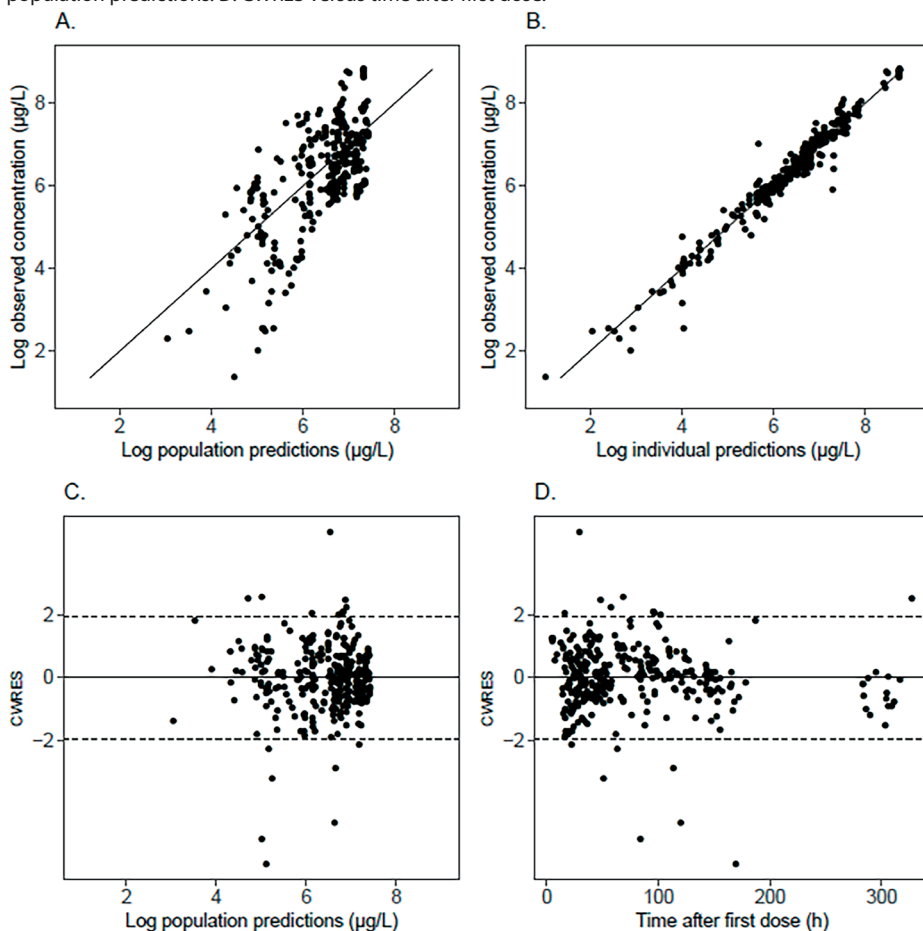




**Figure S3** Normalized prediction distribution error (NPDE) of the final model for oral [ $^{14}\text{C}$ ]midazolam. A. Quantile-quantile plot of NPDE versus the expected standard normal distribution. B. The histogram of NPDE with the observed frequency of sample quantiles of the NPDE (white bars), overlaid with the density of the standard normal distribution (grey bars). C. NPDE versus time, with the NPDE for each observation (dots) and the lines indicating the mean (light grey middle line) and the 90% percentiles (light grey upper and lower line) of the NPDE, and the shaded areas are the simulated 90% confidence intervals of the NPDE median (light grey middle box) and 95% percentiles (light grey upper and lower box). D. NPDE versus predicted concentration, with dots and lines as described for C.

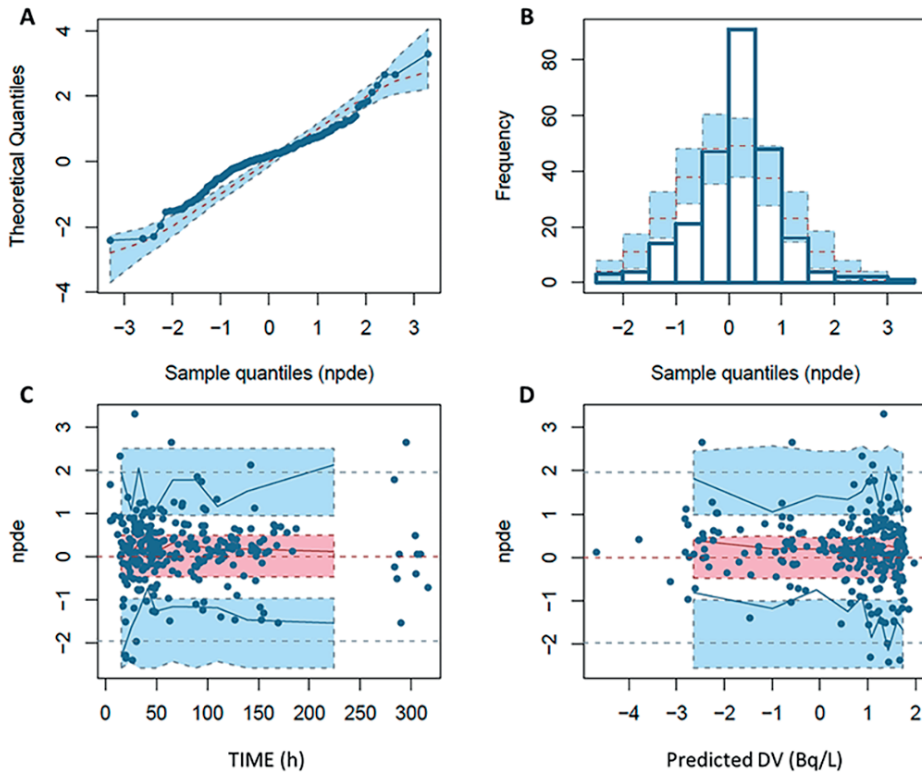


**Figure S4** Normalized prediction distribution error (NPDE) of the final model for intravenous midazolam.

A. Quantile-quantile plot of NPDE versus the expected standard normal distribution. B. The histogram of NPDE with the observed frequency of sample quantiles of the NPDE (white bars), overlaid with the density of the standard normal distribution (grey bars). C. NPDE versus time, with the NPDE for each observation (dots), and the lines indicate the mean (light grey middle line) and the 90% percentiles (light grey upper and lower line) of the NPDE, and the shaded areas are the simulated 90% confidence intervals of the NPDE median (light grey middle box) and 95% percentiles (light grey upper and lower box). D. NPDE versus predicted concentration, with dots and lines as described for C.

